Biofabrication

International Society for Biofabrication

ACCEPTED MANUSCRIPT

High density cell seeding affects the rheology and printability of collagen bioinks

To cite this article before publication: Nicole Diamantides *et al* 2019 *Biofabrication* in press https://doi.org/10.1088/1758-5090/ab3524

High density cell seeding affects the rheology and printability of collagen bioinks

Nicole Diamantides[1], Caroline Dugopolski[2], Eric Blahut[2], Stephen Kennedy[2], and Lawrence J. Bonassar, PhD[1,3]*

[1]Meinig School of Biomedical Engineering, Cornell University, Ithaca, NY
[2]Histogenics Corporation, Waltham, MA
[3]Sibley School of Mechanical and Aerospace Engineering, Cornell University, Ithaca, NY

*Address Correspondence to:
Lawrence J. Bonassar, PhD.
Professor
Department of Biomedical Engineering
149 Weill Hall
Cornell University
Ithaca, NY 14853
(607) 255-9381
lb244@cornell.edu

Key Words: bioprinting, extrusion, collagen, chondrocytes, cell density, cartilage, tissue engineering

Running Title: Chondrocyte bioprinting

Abstract

An advantage of bioprinting is the ability to incorporate cells into the hydrogel bioink allowing for precise control over cell placement within a construct. Previous work found that the printability of collagen bioinks is highly dependent on their rheological properties. The effect of cell density on collagen rheological properties and, therefore, printability has not been assessed. Therefore, the objective of this study was to determine the effects of incorporating cells on the rheology and printability of collagen bioinks. Primary chondrocytes, at densities relevant to cartilage tissue engineering (up to $100x10^6$ cells/mL), were incorporated into 8 mg/mL collagen bioinks. Bioink rheological properties before, during, and after gelation as well as printability were assessed. Cell-laden printed constructs were also cultured for up to 14 days to assess longer-term cell behavior. The addition of cells resulted in an increase in the storage modulus and viscosity of the collagen before gelation. However, the storage modulus after gelation and the rate of gelation decreased with increasing cell density. Theoretical models were compared to the rheological data to suggest frameworks that could be used to predict the rheological properties of cell-laden bioinks. Printability testing showed that improved printability could be achieved with higher cell densities. Fourteen-day culture studies showed that the printing process had no adverse effects on the viability or function of printed cells. Overall, this study shows that collagen bioinks are conducive to bioprinting with a wide range of cell densities while maintaining high printability and chondrocyte viability and function.

1. Introduction

Extrusion bioprinting allows for the incorporation of cells into bioinks and for precise control of cell placement within tissue engineered constructs. Because cells can be mixed directly into the bioink, extrusion bioprinting provides the flexibility to create complex constructs with varying cell densities or different cell types in different regions of the construct [1–3]. Extrusion bioprinting also allows for the creation of geometrically complex constructs with high resolution. However, the print resolution of this process is in part dependent on the properties of the bioink being used.

The print resolution that can be achieved with a given bioink is often measured as a surrogate quantification for bioink printability. The print resolution and, therefore, printability of the bioink are known to be highly dependent on the bioink's rheological properties [4–11]. However, it is unclear what effect the incorporation of cells has on bioink rheological properties. The effect of cells on bioink rheology is of particular importance for extrusion bioprinting where rheological properties prior to gelation are important for print resolution and mechanical properties after gelation are important for implant performance.

Previous studies have shown that the addition of cells has varying effects on a biomaterial's rheological properties. For example, the addition of 1 million cells/mL to gelatin/alginate biomaterials was found to decrease the storage modulus in the gelled state [12]. The addition of cells to gelatin methacrylamide biomaterials also resulted in a decreased storage modulus and viscosity [13]. However, in the non-crosslinked or non-gelled states, the results are less consistent. For example, cell-laden gelatin methacrylamide biomaterials in the non-gelled state exhibit decreased viscosity compared to acellular biomaterials [13]. But, non-crosslinked cell-laden alginate biomaterials exhibit increased viscosity and storage modulus compared to acellular formulations [14]. Only one study has specifically investigated the effects of adding cells to the

printability of a bioink. Adding 1.5 million cells/mL to gelatin methacrylamide resulted in increased diameters of printed struts (i.e. decreased printability) [13].

However, all of these studies on the effect of adding cells to biomaterials have used relatively low cell densities (0.5-10 million cells/mL). Tissue engineering applications utilize a much wider range of cell densities. Cartilage tissue engineering, in particular, has traditionally used a large range of cell densities from 1 million to 100 million cells/mL [15–17]. Cartilage tissue engineering utilizing 25 million cells/mL in a collagen biomaterial has been shown to be effective for producing menisci and auricles [18,19]. Unfortunately, no studies have investigated the effects of cell densities relevant to cartilage tissue engineering, on the order of 25 million to 100 million cells/mL, on the rheological properties of biomaterials or the printability of bioinks.

A common biomaterial for use in cartilage tissue engineering is collagen. Collagen is a promising bioink [20,21] and is well-suited for cartilage tissue engineering due to its natural cell binding sites, ability to be enzymatically degraded, and temperature-dependent gelation. When kept at 4 °C, collagen remains in solution form and can be easily extruded during bioprinting. If the print surface is held at 37 °C, the collagen will form a solid hydrogel upon deposition and maintain the intended bioprinted shape [1]. The printability of collagen bioinks depends on their rheological properties before gelation when the collagen is still in the solution phase [4]. Due to the low viscosity of most collagen bioinks, in several studies, they have been combined with other biomaterials to improve the printability [22,23]. The printability of collagen bioinks can also be improved by increasing the collagen concentration [1]. Unfortunately, few studies have focused on characterizing the rheological properties of high concentration (>5 mg/mL) collagen gels used for cartilage tissue engineering. Further, the effect of adding cells at densities relevant to cartilage tissue engineering on the rheological properties and printability of collagen bioinks is unknown.

Therefore, the first objective of this study was to determine how collagen bioink rheology and printability are affected by the addition of cell densities up to 100 million cells/mL.

Additionally, there is a need for a theoretical model of the rheological properties of cell-laden biomaterials that applies to various cell densities, cell types, and material types that could be used to predict the rheological behavior of cell-laden bioinks. Classical theories of composites have yet to be applied to the rheology of bioink formulations. Therefore, we applied several classical models, including the rule of mixtures, Einstein's formula of viscosity [24], Taylor correction [25], and the Christensen model [26], to our rheological findings to determine which best described the behavior of cell-laden collagen bioinks.

Understanding or predicting how the addition of cells influences the rheological properties and printability of a bioink is only useful if these cells survive and thrive after the bioprinting process. A previous study found that chondrocyte viability remained high after bioprinting with collagen bioinks at a cell density of 10 million cells/mL and collagen concentrations up to 17.5 mg/mL [1]. We therefore expect similar outcomes when bioprinting with an 8 mg/mL collagen bioink with our bioprinter setup. We also want to determine that these chondrocytes are functioning properly after being bioprinted which can be assessed as the ability to remodel the matrix and produce glycosaminoglycans [18]. Therefore, the second objective of this study was to determine how the bioprinting process affects the viability and function of encapsulated chondrocytes.

2. Materials and Methods

2.1 Cell isolation

Chondrocytes were extracted from the cartilage of neonatal bovids as described previously [4,17]. Femoral condyles were chopped and then digested for 16-18 hours in Dulbecco's modified eagle's medium (DMEM, Corning cellgro, Manassas, VA) containing 0.25% collagenase

(Worthington Biochemical Corp, Lakewood, NJ), 100 units/mL penicillin (Corning, Manassas, VA), 100 µg/mL streptomycin (Corning, Manassas, VA), and 0.25 µg/mL amphotericin B (Corning, Manassas, VA). After digestion, the solution was centrifuged, rinsed with 1X phosphate buffered saline (PBS, Corning cellgro, Manassas, VA), and cells were counted using Trypan blue (Corning cellgro, Manassas, VA). Cells were used immediately for rheology and printability testing. For extended culture, cells were first plated on triple flasks with DMEM with 100 units/mL penicillin, 100 µg/mL streptomycin, 0.25 µg/mL amphotericin B, and 10% fetal bovine serum (FBS, Gemini Bio-Products, West Sacramento, CA) for 5-7 days. This allowed the cells to become adherent so that dead cells could be rinsed away. Once adherent, cells were trypsinized (Corning, Manassas, VA) and counted using Trypan blue.

2.2 Bioink preparation

Type I collagen was extracted from the tendons of rat tails (BioreclamationIVT, Westbury, NY) and solubilized in 0.1% acetic acid as previously described [27]. Briefly, isolated tendons were soaked in 0.1% acetic acid (Sigma, St. Louis, MO) at a concentration of 1 g per 150 mL acetic acid for at least 48 hours at 4 °C. This solution was then centrifuged for 90 minutes at 9000 rpm and the resulting supernatant was collected, frozen, and lyophilized for at least 96 hours. Once lyophilized, collagen was reconstituted in 0.1% acetic acid at a concentration of 15 mg/mL to create a stock collagen solution.

Collagen bioinks were prepared by mixing the stock collagen solution with a working solution of 1X PBS, 10X PBS (Corning cellgro, Manassas, VA), and 1 N NaOH (Avantor, Center Valley, PA) and then mixing with the desired number of chondrocytes. The final collagen concentration was 8 mg/mL and the final cell densities were 0, $5x10^6$, $10x10^6$, $25x10^6$, or $100x10^6$ cells/mL corresponding to a cell volume fraction of 0-0.18.

2.3 Rheology

Rheological measurements of collagen bioinks before, during, and after gelation were obtained as previously described [4]. Briefly, 25 mm glutaraldehyde-treated coverslips [28] were attached to the parallel plates of an Anton-Paar MCR 501 rheometer. Testing was performed at 0.1 Hz and 0.5% strain with a 1 mm gap. Collagen bioinks with final cell densities of 0, $5x10^6$, $10x10^6$, $25x10^6$, or $100x10^6$ cells/mL were prepared as described above and then loaded onto the rheometer with mineral oil to prevent dehydration. A time sweep experiment was performed with the storage modulus (G') and loss modulus (G") measured for 5 minutes at 4 °C followed by 30 minutes at 37 °C.

The rheology of polymer solutions used as bioinks is dependent on a wide variety of properties and includes phenomena such as shear thinning, yield stress, and recovery after yield, all of which may affect printability [9,10]. As such, the shear thinning behavior, yield stress, and recovery time of collagen bioinks with varying cell densities were also determined. These tests were performed on the collagen bioink prior to gelation, as this is the state of the bioink when it is extruded during the printing process. These tests were performed on a TA Instruments DHR3 rheometer using glutaraldehyde-coated coverslips attached to the parallel plate geometry. All tests were conducted at 4°C. To determine the shear thinning behavior, a frequency sweep was performed from 0.01 to 10 Hz. The resulting data was fit to the power law equation [10] to determine the consistency index (K) and flow mode (n) of collagen bioinks, where the power law equation is

$$\eta = K\dot{\gamma}^{n-1}$$

and where η is viscosity and $\dot{\gamma}$ is the shear rate. Yield stress was measured by performing a shear stress sweep from 0.01 to 100 Pa. The yield stress was determined as the stress at the intersection between a horizontal line fit to plateau region before yielding and a line fit to the yielding region

[10]. The plateau viscosity was determined as the average viscosity of the plateau region. Recovery time was determined by first applying an oscillatory shear of 0.5% strain and 0.1 Hz for 5 minutes, then applying a flow mode shear at 100 Hz for 10 seconds, and then returning to an oscillatory shear of 0.5% strain and 0.1 Hz for 5 minutes. Recovery time was defined as the amount of time required for the bioink to return to pre-stress viscosity after the 100 Hz shearing stopped.

2.4 Printability

Bioink printability was assessed using a Fab@Home extrusion-based 3D printer (Seraph Robotics, Ithaca, NY). Collagen bioinks were prepared as described above with 0-100x10^6 cells/mL and the addition of 0.01 mg fluorescein (Sigma, St. Louis, MO) to enable high contrast imaging. The solution was then loaded into a 10 mL syringe that was surrounded with ice packs during the printing process to prevent early gelation of the collagen. All printing was performed using a 0.25 mm tapered nozzle (Nordson EFD, East Providence, RI) onto a glass slide held at 37 °C. Continuous lines with alternating directions consisting of 5 vertical struts of 20 mm in length with 5 mm horizontal spacing were printed to show the deposition of continuous filaments with changes in direction. Dots (0.01-0.09 mL) and lines (50 mm length) were printed to assess bioink printability. Images of the dots and lines were acquired under UV light and were analyzed using ImageJ and MATLAB to determine the footprint area of printed dots and average width of printed lines.

2.5 Construct bioprinting

Square (25.0 x 25.0 x 1.5 mm) constructs were printed using the same system described above using 8 mg/mL collagen and 10x10^6 cells/mL. Cell-laden collagen bioinks were loaded into a 10 mL syringe that was surrounded with ice packs during the printing process. Square constructs were printed directly onto a sterile petri dish held at 37 °C that was transferred to an incubator

immediately after printing. Constructs were left in the incubator for 30 minutes to ensure complete gelation and then were covered with DMEM with 200 units/mL penicillin, 200 µg/mL streptomycin, 0.5 µg/mL amphotericin B, and 10% FBS. Constructs were cultured for up to 14 days with media changes every 1-2 days.

2.6 Viability

Chondrocyte viability was assessed on days 0, 1, 3, 7, and 14. Hemicylinder samples were obtained by bisecting 8 mm punches taken from bioprinted squares. These hemicylinder samples were then stained using 0.5 µL calcein AM (Life Technologies, Eugene, OR) and 0.25 µL ethidium homodimer (Life Technologies, Eugene, OR) per 1 mL of 1X PBS for 30 minutes. Samples were then rinsed with 1X PBS for 5 minutes before being imaged using fluorescence microscopy. A cell counting MATLAB code was used to quantify live and dead cells [29].

2.7 Shape retention

Shape retention of bioprinted squares was assessed to determine construct contraction with time in culture. Gross images of bioprinted squares were obtained on days 0, 1, 3, 5, 7, 9, 11, 13, and 14. These images were analyzed using GIMP and ImageJ to determine construct area.

2.8 Biochemistry

Biochemical analyses were performed on day 0, 7, and 14 samples. Hemicylinder samples were obtained by bisecting 8 mm punches taken from bioprinted squares. The resulting hemicylinders were frozen, lyophilized, and weighed to determine dry weight. Samples were then digested in 1 mL of 0.125 mg/mL papain solution for 12-16 hours at 60 °C. After digestion, DNA content was quantified using the Hoechst DNA assay and sulfated glycosaminoglycan (sGAG) content was quantified using a dimethylmethylene blue assay, as previously described [30,31]. DNA and sGAG content are reported as normalized to sample dry weight.

2.9 Statistics

The effects of cell density on rheological properties were assessed using a one-way ANOVA with Tukey HSD post hoc test, except in the case of the storage modulus before gelation where normality and equal variance assumptions were not met. For this case, the effect of cell density was assessed using a Kruskal-Wallis test with Dunn post hoc test with Bonferroni correction with comparisons to acellular controls. The effects of cell density and volume deposited on the printability of printed dots were assessed by one-way ANCOVA. The effect of cell density on the printability of printed lines was determined by one-way ANOVA with Tukey HSD post hoc test. The effect of culture time on viability, shape retention, and biochemical properties were assessed by one-way ANOVA with Tukey HSD post hoc test. Data are reported as mean ± standard deviation unless otherwise stated.

3. Results

3.1 Rheology

From time sweep experiments, 4 parameters of rheological properties were extracted: G' of the bioink before gelation (G'_0), G' of the bioink after complete gelation (G'_∞), the growth rate of G' (dG'/dt), and the crossover time (t_c) (Figure 1). G'_0 was calculated as the average storage modulus during the 5 minutes of testing at 4 °C when the collagen remained in the solution phase. G'_∞ was calculated as the average storage modulus during the final 20 minutes of testing at 37 °C after the collagen had undergone complete gelation. dG'/dt was calculated as the maximum growth rate of the storage modulus after the temperature was raised to 37 °C and the collagen had started to gel. t_c was calculated as the time when the storage modulus surpassed the loss modulus and the collagen transitioned from a liquid to a solid. Parameters for G" followed the same trends as G' and are provided in the supplemental materials (Supp. Figure 1).

Rheological testing showed that the addition of cells to collagen bioinks in the solution phase increased the storage modulus. G' increased from 0.3 Pa for acellular controls to 0.7 Pa for collagen bioinks with 100 million cells/mL, a 133% increase ($p<0.05$ by Kruskal-Wallis test) (Figure 2A). Conversely, the addition of cells decreased the rheological properties of the collagen after gelation. G' after gelation for acellular controls averaged 413 Pa but samples with 100 million cells/mL only reached 314 Pa, a 24% reduction ($p<0.01$ by one-way ANOVA) (Figure 2B). A similar trend was seen for the growth rate of the storage modulus. The growth rate slowed from 5.2 Pa/s for acellular controls to 3.4 Pa/s for collagen bioinks with 100 million cells/mL, a 35% reduction ($p<0.01$ by one-way ANOVA) (Figure 2C). Despite this significant reduction in gelation kinetics, the crossover time of G' and G" did not change significantly with cell density. The crossover time remained between 1.5 and 2 minutes for all conditions tested (Figure 2D).

All collagen bioink formulations exhibited shear thinning behavior regardless of cell density (Figure 3A). At a low frequency (0.01 Hz) bioinks had viscosities around 8 Pa-s and thinned to around 0.7 Pa-s at a high frequency (10 Hz). When these curves were fit to the power law equation, the shear thinning coefficients, K and n, did not vary with cell density (Table 1). Three range values can be defined for n: $n<1$ for shear thinning behavior, $n=1$ for Newtonian behavior, and $n>1$ for shear thickening behavior [32]. For all cell concentrations, n was less than 1 indicating that all bioink formulations displayed shear thinning behavior.

All bioink formulations displayed a yield point with increasing shear stress (Figure 3B). Collagen bioinks yielded at slightly lower stresses with increasing cell density, with acellular bioinks yielding at 1.52 Pa and bioinks with 100 million cells/mL yielding at 0.744 Pa. Additionally, similar to the trend seen in storage modulus before gelation, the viscosity of the bioink at stresses less than the yield stress was greater with increasing cell densities. Acellular

bioinks had a viscosity of 23.0 Pa-s and bioinks with 100 million cells/mL had a viscosity of 43.7 Pa-s, a 90% increase (Table 1).

Collagen bioinks with and without cells exhibited quick recovery following shearing at a high frequency (Figure 3C). Bioinks had viscosities around 7 Pa-s before shearing at a high frequency. The viscosity dropped to around 0.4 Pa-s at a high frequency but quickly recovered to 7 Pa-s when the frequency was lowered to 0.1 Hz. The time to recover did not change much with cell density with all formulations recovering within 10-35 seconds (Table 1).

3.2 Printability

Bioink formulations with cell densities from 0 to 100 million cells/mL were all printed successfully. The ability to print continuous lines with changes in direction was exhibited by all bioink formulations (Figure 4A).

Dot printing showed that the volume extruded was proportional to the resulting footprint areas of printed dots (Figure 4B), which is consistent with a previous study [4]. Printability was assessed, in part, as the amount of spread of printed dots (i.e. dots with smaller areas for a given volume extruded have better printability than those with larger footprint areas).

Dot printing studies using collagen bioinks with varying cell densities showed that the linear relationship between dot footprint area and volume extruded was conserved for all cell densities. Although pairwise comparisons were not statistically different; overall, dots printed with bioinks containing 25 and 100 million cells/mL were smaller in area than those printed with acellular bioinks (Figure 4B). For example, 0.084 mL dots had average footprint areas of 84 mm^2 and 90 mm^2, for 100 million cells/mL and acellular bioinks, respectively. ANCOVA analysis of this data determined that the slopes of the linear fits were the same for all cell densities, but that the intercepts (i.e. the elevation of the curves) for 25 and 100 million cells/mL bioinks were lower

than that of acellular controls ($p<0.05$). These data suggest that finer resolution and improved printability could be achieved with collagen bioinks with higher cell densities. This observation is consistent with a previous study [4] that bioinks with higher storage moduli before gelation result in improved printability.

Line printing studies using collagen bioinks with varying cell densities also showed that high cell densities resulted in improved printing resolution (Figure 4C). Collagen bioinks with cell densities of 5, 25, and 100 million cells/mL resulted in printed lines with significantly smaller widths than those printed with acellular bioinks. Lines printed with acellular bioinks had widths around 1.2 mm whereas lines printed with bioinks containing 100 million cells/mL had widths around 0.8 mm, a 33% improvement in print resolution.

3.3 Viability

Live/dead stains were performed to determine the viability of chondrocytes immediately after bioprinting and up to 14 days in culture. For these tests, all bioprinted constructs were fabricated using collagen bioinks containing 10 million cells/mL. Viability was found to be high (>90%) on day 0 and viability remained high throughout the 14 days in culture (Figure 5). This suggests that the shear stresses applied to the cells during the bioprinting process are not high enough to cause cell death.

3.4 Shape retention

The area of bioprinted constructs was measured throughout the 14 days in culture for constructs fabricated using collagen bioinks containing 10 million cells/mL (Figure 6). The area was generally maintained during the first 9 days in culture with less than 5% change in area from day 0 ($p>0.90$ by one-way ANOVA). However, by days 11 to 14, significant contraction had occurred, resulting in constructs with 84-85% of their initial area ($p<0.01$, compared to day 0 by one-way

ANOVA). This observation is consistent with previous studies demonstrating that embedded chondrocytes actively remodel the collagen matrix during extended in vitro culture [18].

3.5 Biochemistry

The biochemical content of bioprinted constructs was measured on days 0, 7, and 14 for constructs fabricated using collagen bioinks containing 10 million cells/mL. DNA content was found to decrease significantly from day 0 to day 7 and then increase slightly from day 7 to day 14, suggesting that the embedded chondrocytes may be slightly proliferative (Figure 7A). The drop from day 0 to day 7 could be due to the removal of any dead cells. GAG content nearly doubled from day 7 to day 14 from 9.8 μg/mg to 18.4 μg/mg ($p<0.05$ by ANOVA) (Figure 7B). Since the constructs started with no GAG content, this means that the chondrocytes were producing GAGs at a relatively constant rate throughout their time in culture.

4. Discussion

The objectives of this study were to (1) determine how the addition of cells affects the rheology and printability of collagen bioinks and (2) determine how the bioprinting process affects chondrocyte viability and function. Regarding the first objective, this study shows that increasing cell densities results in an increase in the storage modulus and viscosity of the collagen bioink before gelation. Conversely, increasing cell densities were found to decrease the collagen storage modulus in the gel phase. While cell density was found to have little effect on the crossover time, the rate of gelation was found to decrease with increasing cell densities. Cell density also did not influence the shear thinning properties, yield stress, or recovery time of collagen bioinks in the solution phase. Dot and line printing experiments showed that improved printing resolution could be achieved using collagen bioinks with higher cell densities (25 and 100 million cells/mL).

An increase was observed in the storage moduli and viscosity of collagen bioinks before gelation with increasing cell densities. A similar trend was reported for the storage moduli and viscosity of alginate biomaterials in the solution phase [14]. Gelatin/alginate and gelatin methacrylamide biomaterials form a gel when cooled. As such, rheological measurements made at higher temperatures (i.e. before gelation) are analogous to those of collagen before gelation at lower temperatures. Above 22 °C, gelatin/alginate biomaterials exhibited an increased storage modulus with the addition of 1 million cells/mL [12] similar to our findings for collagen. At high temperatures, gelatin methacrylamide biomaterials exhibited a decrease in viscosity with increasing cell densities [13]. This discrepancy could be because the viscosity of gelatin methacrylamide in the solution phase is similar to or greater than that of the encapsulated cells and the storage moduli of collagen, alginate, and gelatin/alginate in the solution phase are less than those of the encapsulated cells.

Collagen bioinks exhibited decreased storage moduli after gelation with increasing cell densities. This trend is similar to the behavior of gelatin/alginate [12] and gelatin methacrylamide [13] biomaterials in the gelled phase. However, no comparison can be made to the pure alginate biomaterial as that study only looked at alginate in the solution phase [14].

Collagen bioinks were also found to have slower gelation rates with higher cell densities. This could be because the cells are physically blocking the binding sites necessary for collagen fiber self-assembly. Gelatin/alginate biomaterials also appear to gel more slowly with the addition of 1 million cells/mL compared to acellular controls [12]. The crossover time was found to vary little with increasing cell densities in collagen bioinks. The crossover point for gelatin methacrylamide biomaterials was found to occur at slightly lower temperatures with increasing cell densities [13],

but the time at which the crossover point occurred was not investigated. These findings suggest that the addition of cells may act to hinder gelation but to only a slight degree.

In comparing these studies, we see that adding cells to a biomaterial generally results in increased rheological properties before gelation, decreased rheological properties after gelation, and slowed gelation, though there are some exceptions. It should also be noted that different cell types were used in each study (chondrocytes in this collagen study, A549 cells in gelatin/alginate [12], fibroblasts in alginate [14], and HepG2 cells in gelatin methacrylamide [13]). This suggests that new bioink formulations with different cell types may need to be tested to determine how they behave with the addition of varying cell densities. Differences in the findings from these studies could be related to the ability of the cells to bind to and interact with the material and to the relative rheological properties of the biomaterials in the solution and gel phases compared to those of the cells themselves. Additionally, different cell types vary in size, so, while the cell density may be held constant, the cell volume fraction may change and the rheological properties are dependent on volume fraction. Therefore, it may be beneficial to report cell volume fraction in addition to cell density.

To better assess how a bioink will behave during printing it is important to fully assess the rheological behavior of the bioink [9,10]. Therefore, we also assessed the shear thinning behavior, yield stress, and recovery time of collagen bioink in the solution phase with varying cell densities. These tests were performed on the bioink in the solution phase because the collagen is in the solution phase when it is printed and extruded through the nozzle and does not start to gel until it has been deposited on the printing surface. All collagen bioink formulations displayed shear thinning behavior with little variation caused by the addition of cells at any concentration. It is important for bioinks to be shear thinning so that they can easily be extruded through a narrow

nozzle during printing and minimize the shear stress experienced by the cells during this process [10]. Yield stress is important for determining how the bioink will start to flow during dispensing and how it will hold its shape after printing. Yield stress testing showed that all collagen bioink formulations yielded around 1 Pa, but that this point decreased slightly with increasing cell densities. The yield point of these collagen bioinks is lower than those of other bioinks [8,10,33], suggesting that it does not take much force to start dispensing, but that collagen bioinks are also easily deformed after printing. But it is important to note that once the collagen bioink is deposited on the print surface, which is held at 37 °C, the collagen begins to gel and the yield point would increase, allowing for improved shape retention and layer stacking. Bioinks also need fast recovery times to quickly return to their zero shear viscosity once deposited on the printing surface, which helps to minimize the spread of the bioink on the surface and improve shape fidelity [9,10]. Collagen bioinks were found to recover their zero-shear viscosity within 10-35 seconds at 4 °C. But in the actual printing setup, the collagen bioink is deposited onto a 37 °C surface and the crossover time of the storage and loss moduli of these bioinks was found to be within 90-120 seconds, so the zero-shear viscosity may be recovered even faster after printing than in the rheological test due to the addition of thermal gelation.

Several studies have investigated how the printability of bioinks is related to various rheological properties and how rheological properties can be used to predict printability [8–11,34]. A previous study from our group found that, for collagen bioinks specifically, the initial storage modulus of the bioink is a good predictor of printability [4]. This current study found that the initial storage modulus of collagen bioinks increased slightly with increasing cell density. Based on the findings of the previous study, we expected dots and lines printed with higher cell densities to have improved printability as exhibited by smaller footprint areas and line widths, respectively, than

acellular collagen bioinks. Dot printing experiments showed that the footprint area of dots did not change significantly with cell density, but the elevation of linear trends predicts that collagen bioinks with higher cell densities exhibit better printability and resolution than acellular collagen bioinks. Line printing experiments showed that collagen bioinks with high cell densities resulted in significantly thinner lines and better print resolution than acellular collagen bioinks. This supports the findings of our former study that the storage modulus before gelation can be used as an indicator of collagen bioink printability. This previous study found that a nearly 20-fold increase in storage modulus before gelation resulted in an approximately 25% decrease in dot footprint area. This current study found a 2.3-fold increase in storage modulus before gelation resulted in an approximately 10% decrease in dot footprint area. This may suggest that the relationship between storage modulus before gelation and footprint area is nonlinear with the same change in storage modulus having a larger effect on footprint area at lower moduli than at higher moduli.

We compared our rheological results to several models of composite materials to determine if the rheological properties of cell-laden collagen bioinks could be predicted. We evaluated these models assuming chondrocytes to have an average diameter of 15 μm [35–38] which is consistent with our histological findings (Supp. Figure 2) and an average storage modulus at 0.1 Hz of 60 Pa [39,40]. Based on the geometry of the cells, this corresponds to cell volume fractions of 0-0.18 for cell densities of 0 to 100 million cells/mL. We found that rheological properties of cell-laden collagen hydrogels before gelation (i.e. in the solution phase) were best predicted by the Einstein equation for viscosity (Figure 8A). The Einstein model is used to determine the viscosity of a dilute suspension of small particles as follows:

$$\eta_c = \eta_m \left(1 + \frac{5}{2} V_p\right)$$

where η_c is the complex viscosity of the composite (cell-laden collagen solution), η_m is the complex viscosity of the matrix (collagen solution alone), and V_p is the volume fraction of the particles (cells). In the solution phase, the chondrocytes act as hard inclusions because the cells are stiffer than the collagen in the solution phase and, therefore, we expected the rheological properties of cell-laden collagen in the solution phase to increase with increasing cell density. The Einstein theory also predicts that viscosity will increase with increasing cell volume fraction. The model predicts that the complex viscosity of collagen bioinks with 100 million cells/mL in the solution phase should be 2.16 Pa-s or 44% more viscous than acellular collagen bioinks. The actual complex viscosity of collagen bioinks with 100 million cells/mL in the solution phase was found to be 2.45 Pa-s or 63% more viscous than the acellular collagen bioinks. The experimental results for the complex viscosity of cell-laden collagen bioinks in the solution phase were within 11-53% of the predicted model values.

Experimentally, we found that the storage modulus of collagen bioinks after gelation decreased with increasing cell densities. We expected a decreasing trend because the cells are less stiff than the gelled collagen matrix and, therefore, act to decrease the modulus of the composite cell-laden collagen. For lower cell densities (5-25 million cells/mL) this trend was best predicted by the isostress rule of mixtures, also known as the lower bound of the rule of mixtures. The isostress rule of mixtures predicts the storage modulus of a composite material as follows:

$$G'_c = \frac{G'_m G'_p}{G'_p V_m + G'_m V_p}$$

Where G'_c is the storage modulus of the composite (cell-laden collagen gel), G'_m is the storage modulus of the matrix (collagen gel alone), G'_p is the storage modulus of the particle (cell), V_m is the volume fraction of the matrix, and V_p is the volume fraction of the particles. The isostress rule predicts a storage modulus of 328 Pa for collagen bioinks containing 25 million cells/mL, or 21%

lower than that of acellular controls (Figure 8B). For cell densities of 5-25 million cells/mL, the experimental values of storage moduli for cell-laden collagen bioinks were within 9% of the values predicted by the isostress rule. However, for collagen containing 100 million cells/mL, the isostress rule predicted a storage modulus of 202 Pa. The experimental result was more than 50% greater than this prediction. The isostrain rule of mixtures, also known as the upper bound of the rule of mixtures, predicted a storage modulus of 350 Pa for collagen containing 100 million cells/mL. The experimental result was within 11% of this prediction. The isostrain rule of mixtures predicts the storage modulus of a composite as follows:

$$G'_c = G'_m V_m + G'_p V_p$$

Therefore, we propose that for lower cell densities, up to 0.05 particle volume fraction, the isostress rule of mixtures is the best predictor of cell-laden bioink rheological properties after gelation and the isostrain rule of mixtures should be used for higher cell densities (around 0.18 volume fraction). This divergence should be considered when either printing with a pre-gelled collagen bioink or when handling and manipulating printed collagen constructs. At cell densities where the isostress rule is a better predictor, the cells could be experiencing larger strains than those imposed on the entire system which could adversely affect cell viability and/or function.

The experimental rheological data was fit to existing models with moderate success. These models (Einstein and rule of mixtures) were found to predict the experimental data quantitatively, as the experimental results are all within 53% of model predictions, with most results within 15% of model predictions. However, these models failed to predict the overall trends and the shape of the model curves do not match the data well. As such, existing models may not be the best way to describe the effect of cell density on rheological properties. There remains a need for a new and better framework that can predict these relationships and trends more accurately.

Cell viability and function are critical to any bioprinted construct. Therefore, the second objective of this study was to determine the effect of the bioprinting process on chondrocyte viability and function. Because storage modulus before gelation was shown to be relatively independent of cell density, a cell density of 10 million cells/mL was used for the second objective. For this objective, 25.0 x 25.0 x 1.5 mm solid squares were printed. This shape was chosen to represent a potential repair for articular cartilage. Solid tissue engineered constructs are often used for cartilage repair because cartilage tissue is avascular and implanted constructs do not need a vascular network to maintain tissue health.

Chondrocyte viability was found to be high (>90%) immediately after printing and up to 14 days in culture. Chondrocytes remodeled the collagen matrix of the constructs after 14 days in culture, with significant construct contraction occurring by day 11. The chondrocytes were found to be slightly proliferative as evidenced by a slight increase in construct DNA content from day 7 to day 14. The chondrocytes deposited new cartilage matrix throughout the time in culture. The GAG content, a primary component of cartilage extracellular matrix, was found to nearly double from day 7 to day 14, suggesting that the chondrocytes are metabolically active.

Several studies have investigated the effect of bioprinting on the viability of encapsulated cells [1,5,12,13,41–43]. These studies have investigated the effects of bioink formulation [1,5], cell concentration [43], temperature [5,12], pressure [13,41–43], and nozzle geometry [13,41,43]. Relationships have been found between cell viability and bioink storage modulus [12] and between cell viability and shear stress [5]. Based on these findings, we can assume that we would find similar cell viabilities using other cell densities in our collagen bioinks. This assumption results from the fact that we found only a small change in the storage modulus of our bioink with higher cell densities. Therefore, if we maintain the same printing parameters and nozzle geometry during

bioprinting, cells should be subjected to similar shear stresses regardless of cell density (up to 100 million cells/mL) and would exhibit the same high cell viabilities. One study found lower cell viabilities when bioprinting with 10 million cells/mL as compared to 0.1 and 1 million cells/mL [43]. However, this effect was only observed on day 3 and no differences in cell viability were seen on day 0 so the viability problems may have been caused by factors after the bioprinting process. Also, this study utilized 3 mg/mL collagen bioinks which may have exhibited a greater change in storage modulus due to the incorporation of cells, but no rheological experiments were performed to confirm this.

Due to the low viscosity of the collagen bioink before gelation, sedimentation of cells within the syringe before printing could be a problem. Xu et al. found that cells in sodium alginate bioinks fall to the bottom of the reservoir more quickly in low viscosity bioinks [44]. This suggests that the density of chondrocytes within our bioink may not be uniform, particularly if left in the syringe for extended periods of time. However, for this study, the squares were printed in under 5 minutes which was likely fast enough to prevent significant sedimentation after mixing. This is also supported by the generally uniform distribution of cells observed in histological imaging of printed constructs (Supp. Figure 2).

Several studies have characterized the longer-term behavior and function of chondrocytes after bioprinting [22,45–49]. These studies found that primary chondrocytes remained viable and maintained their function after bioprinting in a variety of bioinks with varying cell densities using different bioprinters. Here, we found that chondrocytes remained viable and remodeled the matrix throughout the 14 days in culture. This was demonstrated by significant contraction after 11 days in culture and a nearly two-fold increase in GAG content from day 7 to day 14. Our study adds to

the literature that suggests that primary chondrocytes are amenable to bioprinting and that cartilage tissue engineering can utilize bioprinting fabrication methods.

5. Conclusions

Overall, this study shows that collagen bioinks are conducive to bioprinting with a wide range of cell densities while maintaining high printability and chondrocyte viability and function. This study found that cell densities up to 100 million cells/mL resulted in increased storage moduli and viscosity of collagen bioinks before gelation, decreased storage moduli of collagen bioinks after gelation, and decreased rates of gelation. Bioinks containing 100 million cells/mL have smaller dot footprint areas and smaller line widths than acellular bioinks, suggesting that increased cell densities could improve bioink printability. Bioprinted constructs showed high cell viability throughout 14 days in culture. These embedded chondrocytes remained active and functional after bioprinting as seen by construct contraction and increased GAG content. This study supports the use of collagen bioinks for cartilage tissue bioprinting. Additionally, this work suggests theoretical models that can be used to predict the rheological properties of cell-laden bioinks to expedite the testing of new bioink formulations regardless of cell or material type.

Acknowledgments

This work was partially funded by an award from Histogenics Corporation to Cornell University. This work made use of the Energy Systems Institute shared research facilities at Cornell University. This work made use of the Cornell Center for Materials Research Shared Facilities which are supported through the NSF MRSEC program (DMR-1719875).

References

[1] Rhee S, Puetzer J L, Mason B, Reinhart-King C A and Bonassar L J 2016 3D Bioprinting of spatially heterogeneous collagen constructs for cartilage tissue engineering *ACS*

Biomater. Sci. Eng. **2** 1800–5

[2] Kolesky D B, Truby R L, Gladman A S, Busbee T A, Homan K A and Lewis J A 2014 3D Bioprinting of Vascularized, Heterogeneous Cell-Laden Tissue Constructs *Adv. Mater.* **26** 3124–30

[3] Jiang T, Munguia-Lopez J G, Flores-Torres S, Grant J, Vijayakumar S, Leon-Rodriguez A De and Kinsella J M 2017 Directing the Self-assembly of Tumour Spheroids by Bioprinting Cellular Heterogeneous Models within Alginate/Gelatin Hydrogels *Sci. Rep.* **7** 4575

[4] Diamantides N, Wang L, Pruiksma T, Siemiatkoski J, Dugopolski C, Shortkroff S, Kennedy S and Bonassar L J 2017 Correlating rheological properties and printability of collagen bioinks: the effects of riboflavin photocrosslinking and pH *Biofabrication* **9** 034102

[5] Ouyang L, Yao R, Zhao Y and Sun W 2016 Effect of bioink properties on printability and cell viability for 3D bioplotting of embryonic stem cells *Biofabrication* **8**

[6] Jia J, Richards D J, Pollard S, Tan Y, Rodriguez J, Visconti R P, Trusk T C, Yost M J, Yao H, Markwald R R and Mei Y 2014 Engineering alginate as bioink for bioprinting *Acta Biomater.* **10** 4323–31

[7] Li H, Liu S and Lin L 2016 Rheological study on 3D printability of alginate hydrogel and effect of graphene oxide *Int. J. Bioprinting* **2** 54–66

[8] Townsend J M, Beck E C, Gehrke S H, Berkland C J and Detamore M S 2019 Flow behavior prior to crosslinking: The need for precursor rheology for placement of hydrogels in medical applications and for 3D bioprinting *Prog. Polym. Sci.* **91** 126–40

[9] Zhang Z, Jin Y, Yin J, Xu C, Xiong R, Christensen K, Ringeisen B R, Chrisey D B and

Huang Y 2018 Evaluation of bioink printability for bioprinting applications *Appl. Phys. Rev.* **5** 041304

[10] Paxton N C, Smolan W, Böck T, Melchels F P W, Groll J and Juengst T 2017 Proposal to Assess Printability of Bioinks for Extrusion-Based Bioprinting and Evaluation of Rheological Properties Governing Bioprintability *Biofabrication*

[11] Yin J, Zhao D and Liu J 2019 Trends on physical understanding of bioink printability *Bio-Design Manuf.* **2** 50–4

[12] Zhao Y, Li Y, Mao S, Sun W and Yao R 2015 The influence of printing parameters on cell survival rate and printability in microextrusion-based 3D cell printing technology *Biofabrication* **7**

[13] Billiet T, Gevaert E, De Schryver T, Cornelissen M and Dubruel P 2014 The 3D printing of gelatin methacrylamide cell-laden tissue-engineered constructs with high cell viability *Biomaterials* **35** 49–62

[14] Xu C, Zhang M, Huang Y, Ogale A, Fu J and Markwald R R 2014 Study of droplet formation process during drop-on-demand inkjetting of living cell-laden bioink *Langmuir* **30** 9130–8

[15] Diduch D R, Jordan L C M, Mierisch C M and Balian G 2000 Marrow stromal cells embedded in alginate for repair of osteochondral defects *Arthrosc. J. Arthrosc. Relat. Surg.* **16** 571–7

[16] Puelacher W C, Kim S W, Vacanti J P, Schloo B, Mooney D and Vacanti C A 1994 Tissue-engineered growth of cartilage: the effect of varying the concentration of chondrocytes seeded onto synthetic polymer matrices *Int. J. Oral Maxillofac. Surg.* **23** 49–53

[17] Chang S C N, Rowley J A, Tobias G, Genes N G, Roy A K, Mooney D J, Vacanti C A and Bonassar L J 2001 Injection molding of chondrocyte/alginate constructs in the shape of facial implants *J. Biomed. Mater. Res.* **55** 503–11

[18] Puetzer J L and Bonassar L J 2013 High density type I collagen gels for tissue engineering of whole menisci *Acta Biomater.* **9** 7787–95

[19] Reiffel A J, Kafka C, Hernandez K A, Popa S, Perez J L, Zhou S, Pramanik S, Brown B N, Ryu W S, Bonassar L J and Spector J A 2013 High-Fidelity Tissue Engineering of Patient-Specific Auricles for Reconstruction of Pediatric Microtia and Other Auricular Deformities ed X He *PLoS One* **8** e56506

[20] Drzewiecki K E, Malavade J N, Ahmed I, Lowe C J and Shreiber D I 2017 A thermoreversible, photocrosslinkable collagen bio-ink for free-form fabrication of scaffolds for regenerative medicine *TECHNOLOGY* 1–11

[21] Kim Y B, Lee H and Kim G H 2016 A strategy to achieve highly porous/biocompatible macroscale blocks using a collagen/genipin bioink and an optimal 3D printing process *ACS Appl. Mater. Interfaces* **8** 32230–40

[22] Yang X, Lu Z, Wu H, Li W, Zheng L and Zhao J 2017 Collagen-alginate as bioink for three-dimensional (3D) cell printing based cartilage tissue engineering *Mater. Sci. Eng. C*

[23] Kreimendahl F, Köpf M, Thiebes A L, Duarte Campos D F, Blaeser A, Schmitz-Rode T, Apel C, Jockenhoevel S and Fischer H 2017 Three-Dimensional Printing and Angiogenesis: Tailored Agarose-Type I Collagen Blends Comprise Three-Dimensional Printability and Angiogenesis Potential for Tissue-Engineered Substitutes *Tissue Eng. Part C Methods* **23** 604–15

[24] Batchelor G K 2002 *An Introduction to Fluid Dynamics* vol 76 (Cambridge UK:

Cambridge University Press)

[25] Taylor G I 1932 The viscosity of a fluid containing small drops of another fluid *Proc. R. Soc.* **138**

[26] Christensen R M 1991 *Mechanics of Composite Materials* (Malabar, Florida: Krieger Publishing Company)

[27] Cross V L, Zheng Y, Won Choi N, Verbridge S S, Sutermaster B A, Bonassar L J, Fischbach C and Stroock A D 2010 Dense type I collagen matrices that support cellular remodeling and microfabrication for studies of tumor angiogenesis and vasculogenesis in vitro *Biomaterials* **31** 8596–607

[28] Hall M S, Alisafaei F, Ban E, Feng X, Hui C-Y, Shenoy V B and Wu M 2017 Fibrous nonlinear elasticity enables positive mechanical feedback between cells and ECMs *Proc. Natl. Acad. Sci. U. S. A.* **113** 14043–8

[29] Bartell L R, Bonassar L J and Cohen I 2017 A watershed-based algorithm to segment and classify cells in fluorescence microscopy images

[30] Kim Y-J, Sah R L Y, Doong J-Y H and Grodzinsky A J 1988 Fluorometric assay of DNA in cartilage explants using Hoechst 33258 *Anal. Biochem.* **174** 168–76

[31] Enobakhare B O, Bader D L and Lee D A 1996 Quantification of Sulfated Glycosaminoglycans in Chondrocyte/Alginate Cultures, by Use of 1,9-Dimethylmethylene Blue *Anal. Biochem.* **243** 189–91

[32] Zhou M, Lee B H, Tan Y J and Tan L P 2019 Microbial transglutaminase induced controlled crosslinking of gelatin methacryloyl to tailor rheological properties for 3D printing *Biofabrication* **11** 025011

[33] Kiyotake E A, Douglas A W, Thomas E E and Detamore M S 2019 Development and

Quantitative Characterization of the Precursor Rheology of Hyaluronic acid Hydrogels for Bioprinting *Acta Biomater.*

[34] Mouser V H M, Melchels F P W, Visser J, Dhert W J A, Gawlitta D and Malda J 2016 Yield stress determines bioprintability of hydrogels based on gelatin-methacryloyl and gellan gum for cartilage bioprinting *Biofabrication* **8** 38004

[35] Jones W R, Ting-Beall H P, Lee G M, Kelley S S, Hochmuth R M and Guilak F 1999 Alterations in the Young's modulus and volumetric properties of chondrocytes isolated from normal and osteoarthritic human cartilage. *J. Biomech.* **32** 119–27

[36] Freitas Jr R A 1999 Cytometrics *Nanomedicine, Vol I: Basic Capabilities* (Georgetown: Landes Bioscience)

[37] Sasazaki Y, Seedhom B B and Shore R 2008 Morphology of the bovine chondrocyte and of its cytoskeleton in isolation and in situ: are chondrocytes ubiquitously paired through the entire layer of articular cartilage? *Rheumatology* **47** 1641–6

[38] Hirsch M S, Cook S C, Killiany R and Hartford Svoboda K K 1996 Increased cell diameter precedes chondrocyte terminal differentiation, whereas cell-matrix attachment complex proteins appear constant *Anat. Rec.* **244** 284–96

[39] Hiratsuka S, Mizutani Y, Tsuchiya M, Kawahara K, Tokumoto H and Okajima T 2009 The number distribution of complex shear modulus of single cells measured by atomic force microscopy *Ultramicroscopy* **109** 937–41

[40] Maksym G N, Fabry B, Butler J P, Navajas D, Tschumperlin D J, Laporte J D and Fredberg J J 2000 Mechanical properties of cultured human airway smooth muscle cells from 0.05 to 0.4 Hz *J. Appl. Physiol.* **89** 1619–32

[41] Nair K, Gandhi M, Khalil S, Yan K C, Marcolongo M, Barbee K and Sun W 2009

Characterization of cell viability during bioprinting processes *Biotechnol. J.* **4** 1168–77

[42] Chung J H Y, Naficy S, Yue Z, Kapsa R, Quigley A, Moulton S E and Wallace G G 2013 Bio-ink properties and printability for extrusion printing living cells *Biomater. Sci.* **1** 763

[43] Smith C M, Christian J J, Warren W L and Williams S K 2007 Characterizing Environmental Factors that Impact the Viability of Tissue-Engineered Constructs Fabricated by a Direct-Write Bioassembly Tool *Tissue Eng.* **13** 373–83

[44] Xu H, Zhang Z and Xu C 2019 Sedimentation study of bioink containing living cells *J. Appl. Phys.* **125** 114901

[45] Cohen D L, Malone E, Lipson H and Bonassar L J 2006 Direct freeform fabrication of seeded hydrogels in arbitrary geometries. *Tissue Eng.* **12** 1325–35

[46] Goldstein T A, Epstein C J, Schwartz J, Krush A, Lagalante D J, Mercadante K P, Zeltsman D, Smith L P and Grande D A 2016 Feasibility of Bioprinting with a Modified Desktop 3D Printer *Tissue Eng. Part C Methods* **22** 1071–6

[47] Xu T, Binder K W, Albanna M Z, Dice D, Zhao W, Yoo J J and Atala A 2013 Hybrid printing of mechanically and biologically improved constructs for cartilage tissue engineering applications *Biofabrication* **5** 015001

[48] Cui X, Breitenkamp K, Finn M G, Lotz M and D'Lima D 2012 Direct Human Cartilage Repair Using 3D Bioprinting Technology *Tissue Eng.* **18** 1304–12

[49] Izadifar Z, Chang T, Kulyk W, Chen X and Eames B F 2016 Analyzing Biological Performance of 3D-Printed, Cell-Impregnated Hybrid Constructs for Cartilage Tissue Engineering *Tissue Eng. Part C Methods* **22** 173–88

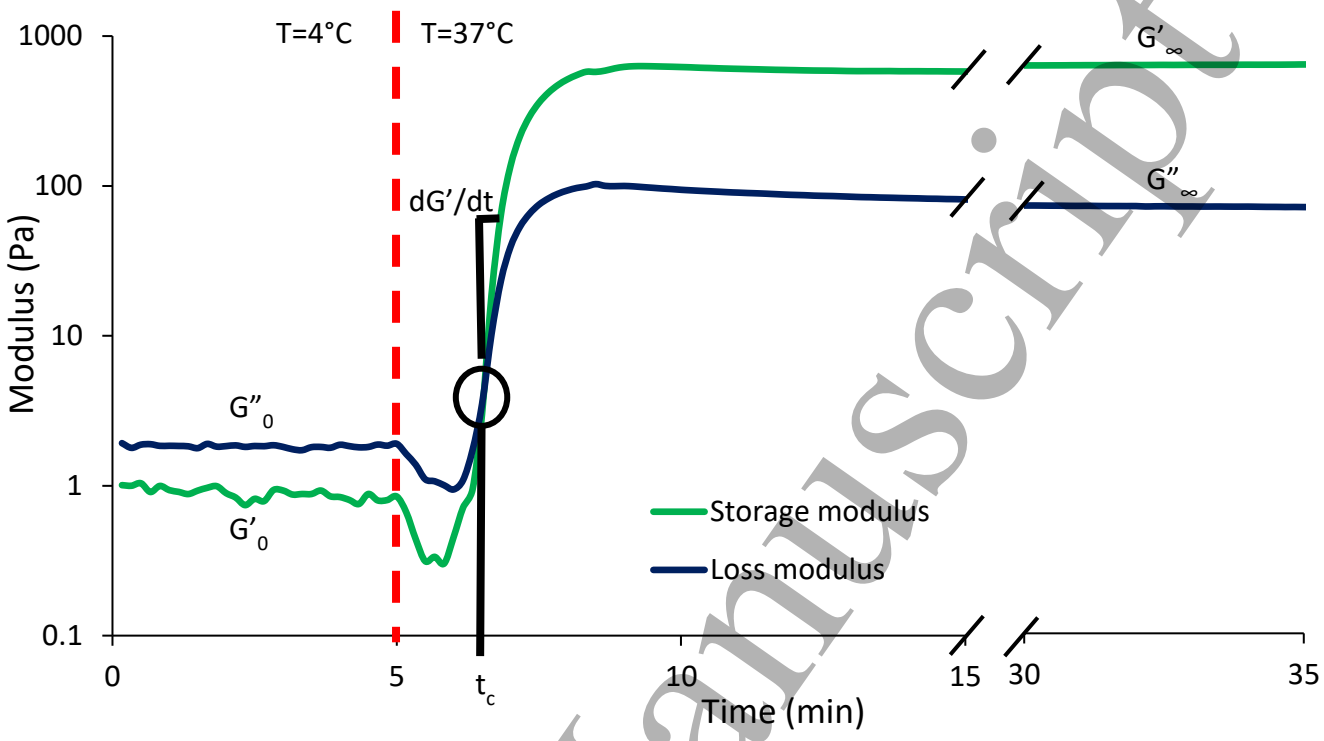

Figure 1. Representative results of rheological testing of 8 mg/mL collagen bioinks. Labels indicate how outcome measures were determined.

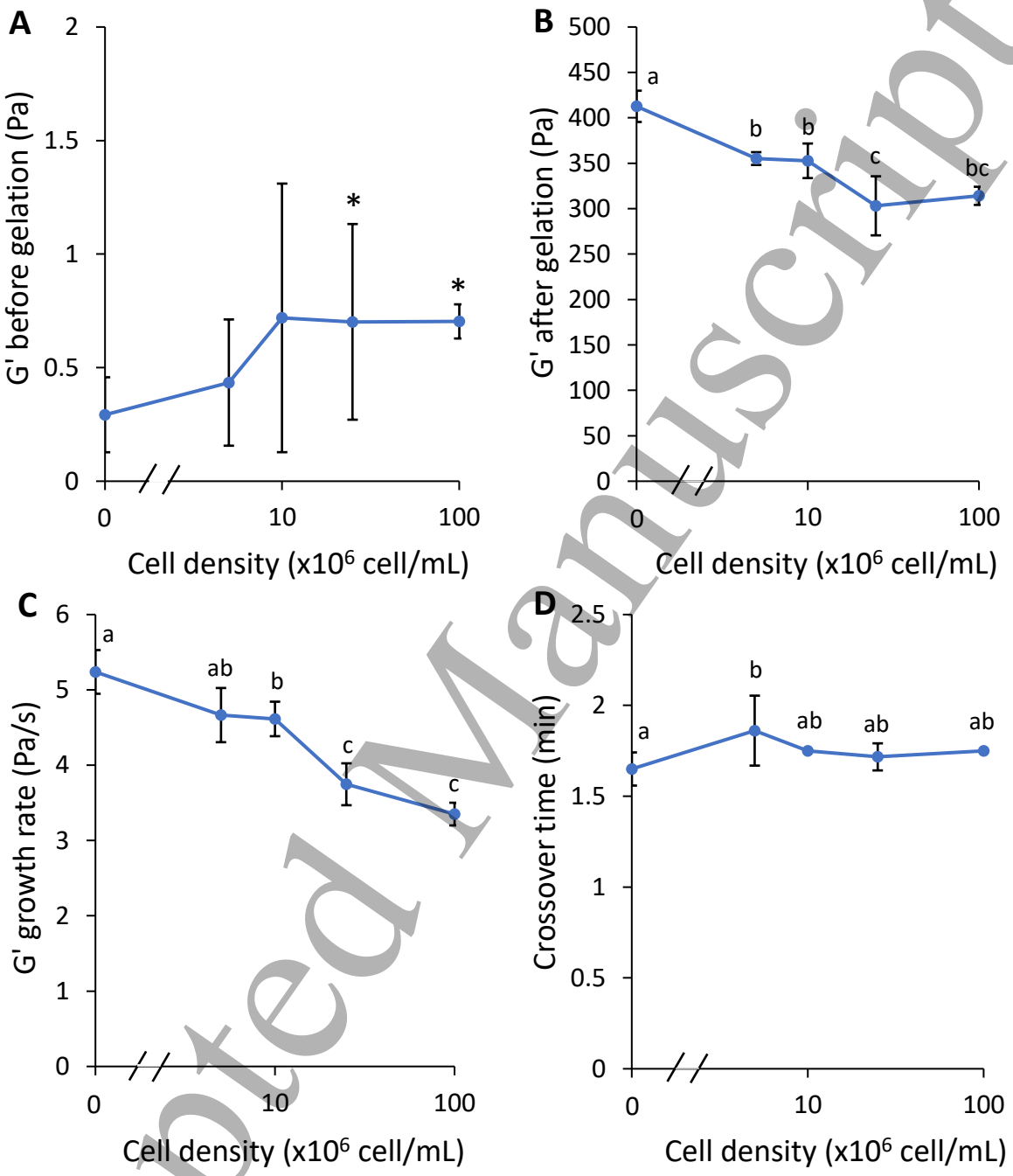

Figure 2. Rheological properties of collagen bioinks before, during, and after temperature-induced gelation with cell densities of 0, 5, 10, 25, and 100 million cells/mL. A.) G' of bioink at 4 °C before gelation. B.) G' of bioink after complete gelation at 37 °C. C.) Maximum growth rate of G' after the temperature was increased to 37 °C. D.) Crossover time of G' and G" after the temperature was increased to 37 °C. n = 3-7 for each group. * indicates significant difference from acellular controls ($p<0.05$ by Kruskal-Wallis for A). Different letters indicate significant differences ($p<0.05$ by one-way ANOVA for B, C, and D).

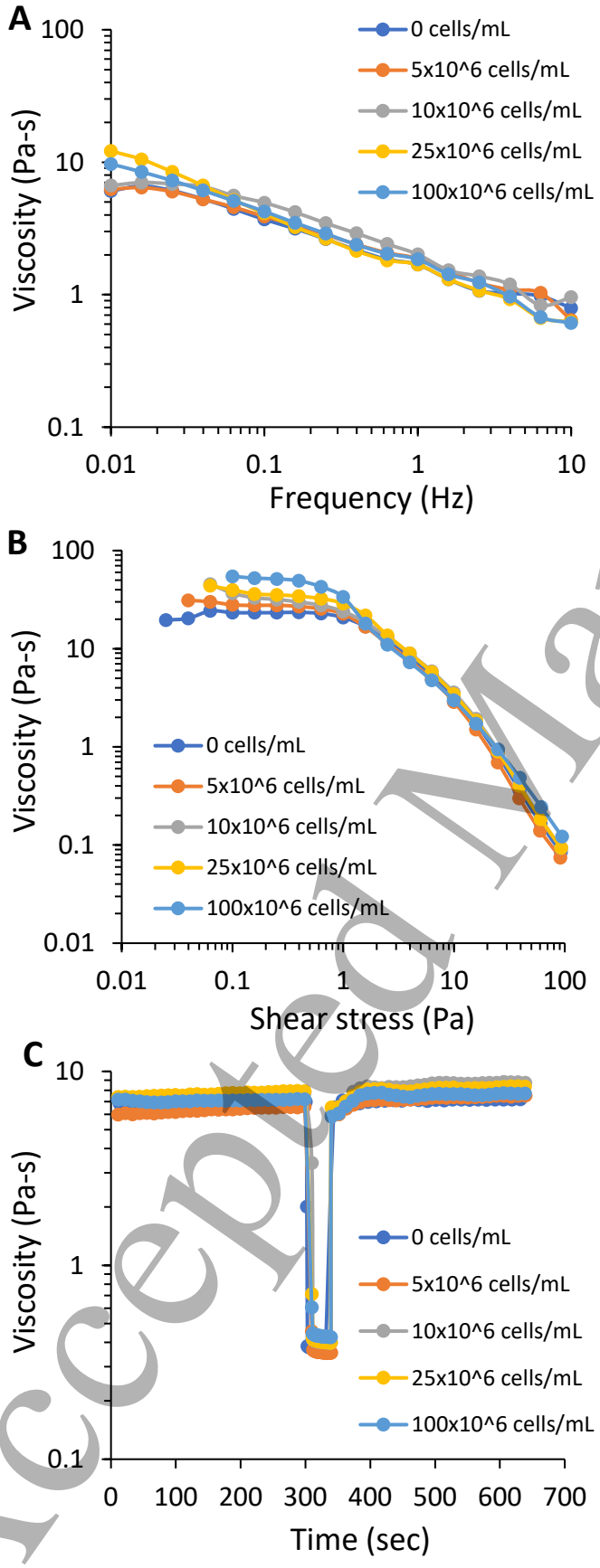

Figure 3. Rheological characterization of collagen bioinks in solution state with cell densities of 0, 5, 10, 25, and 100 million cells/mL. A.) Representative data of bioink shear thinning behavior from 0.01 to 10 Hz. B.) Representative data of bioink yield stress. C.) Representative data of bioink recovery time.

Table 1. Summary of bioink rheological characterization for collagen bioinks with cell densities of 0, 5, 10, 25, and 100 million cells/mL. K and n are shear thinning coefficients derived by fitting the data in the viscosity versus frequency plots to the power law equation. Yield stress was determined as the stress at the intersection between the plateau region and linear region of the viscosity versus shear stress plots. Plateau viscosity is the average viscosity of the plateau region of the viscosity versus shear stress plots. Recovery time is the time for the bioink to return to pre-stress viscosity after shearing at 100 Hz was stopped and the frequency was returned to 0.1 Hz. n=3 tests per cell concentration.

Cell concentration ($x10^6$ cells/mL)	K	n	Yield stress (Pa)	Plateau viscosity (Pa-s)	Recovery time (sec)
0	1.64 ± 0.14	0.715 ± 0.026	1.52 ± 0.24	23.0 ± 2.2	20.5 ± 6.8
5	1.80 ± 0.20	0.720 ± 0.018	1.47 ± 0.02	29.8 ± 6.2	14.0 ± 5.2
10	2.30 ± 0.03	0.693 ± 0.032	1.46 ± 0.03	36.2 ± 8.4	27.4 ± 15.0
25	1.36 ± 0.26	0.435 ± 0.206	1.32 ± 0.12	39.8 ± 6.7	31.1 ± 17.4
100	2.16 ± 0.77	0.623 ± 0.175	0.744 ± 0.050	43.7 ± 5.6	29.5 ± 16.4

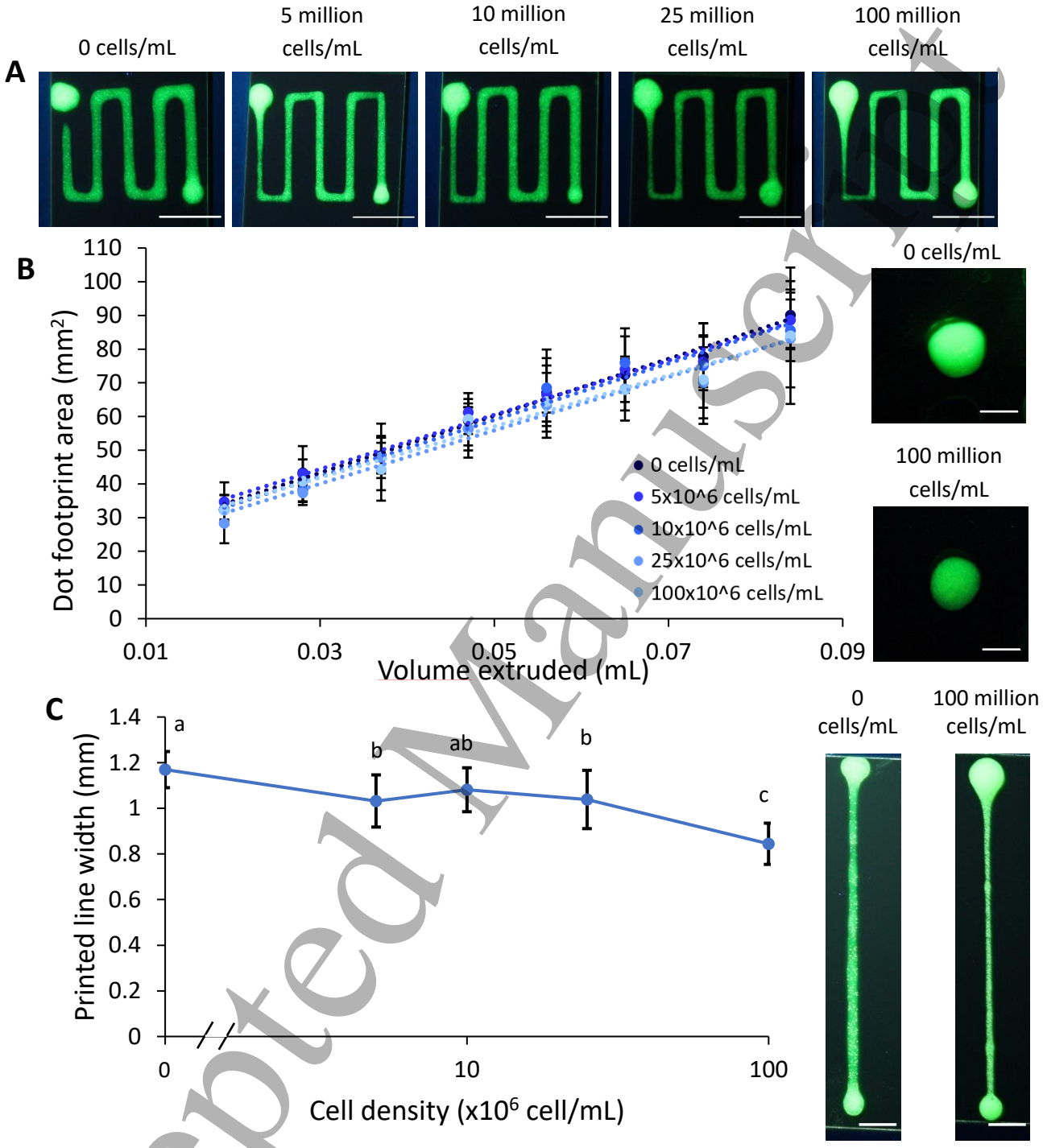

Figure 4. Printability measures of collagen bioinks with cell densities of 0, 5, 10, 25, and 100 million cells/mL. A.) Representative images of printed constructs showing deposition of continuous filament. Scale bar = 10 mm. B.) Footprint areas of printed dots. n = 7-8 for each group. Linear models showed no difference in the slopes of fitted lines but did show that intercepts for 25 and 100 million cells/mL groups were significantly lower than that of acellular controls ($p<0.05$). Top inset shows representative dot printed with 0 cells/mL and bottom inset shows representative dot printed with 100 million cells/mL. Both dots were printed with the same extrusion volume. Scale bars = 5 mm. C.) Widths of printed lines. n=10-17 for each group. Different letters indicate significant differences ($p<0.05$). Left inset

shows representative line printed with 0 cells/mL and right inset shows representative line printed with 100 million cells/mL. Scale bars = 5 mm.

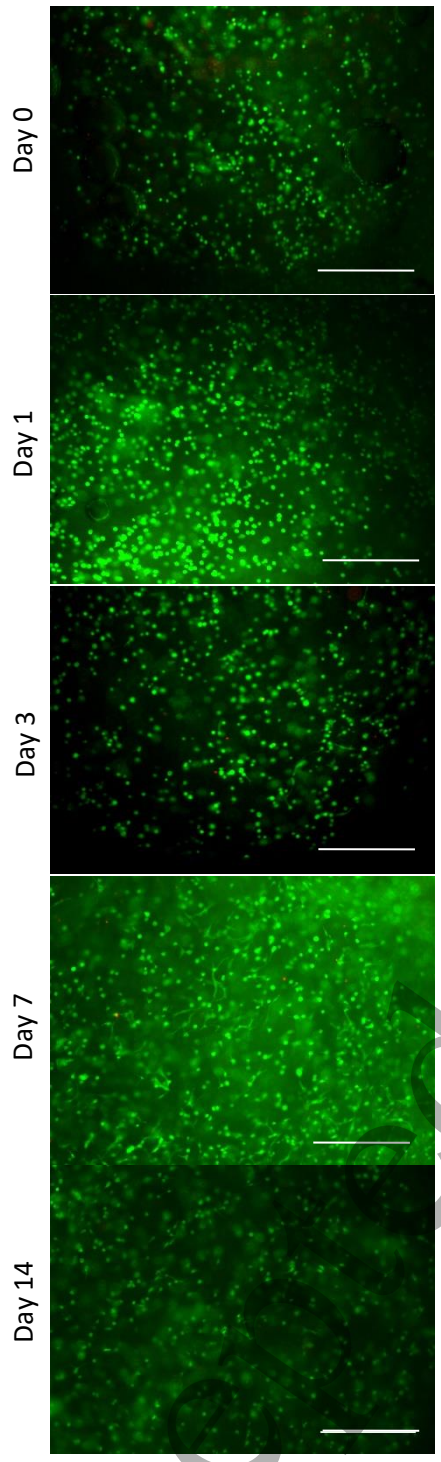

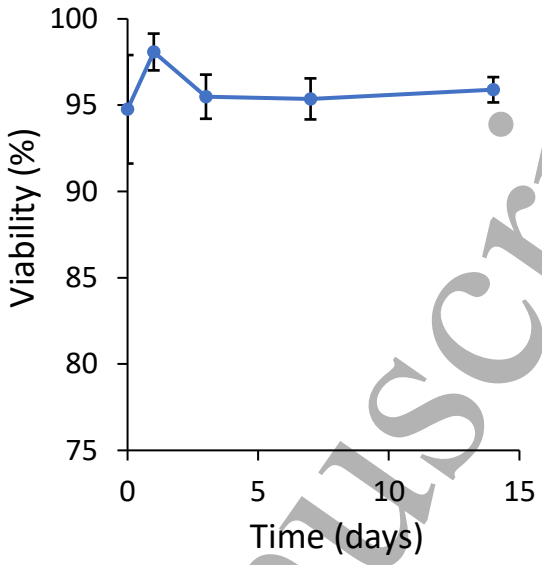

Figure 5. Chondrocyte viability in collagen bioprinted constructs after bioprinting. All samples fabricated using collagen bioinks with 10 million cells/mL. n = 3-8 samples per time point. No significant differences were found. Left panel shows representative images of live/dead stains for day 0, 1, 3, 7, and 14 constructs. Live cells are stained green and dead cells are stained red. Scale bars = 0.5 mm.

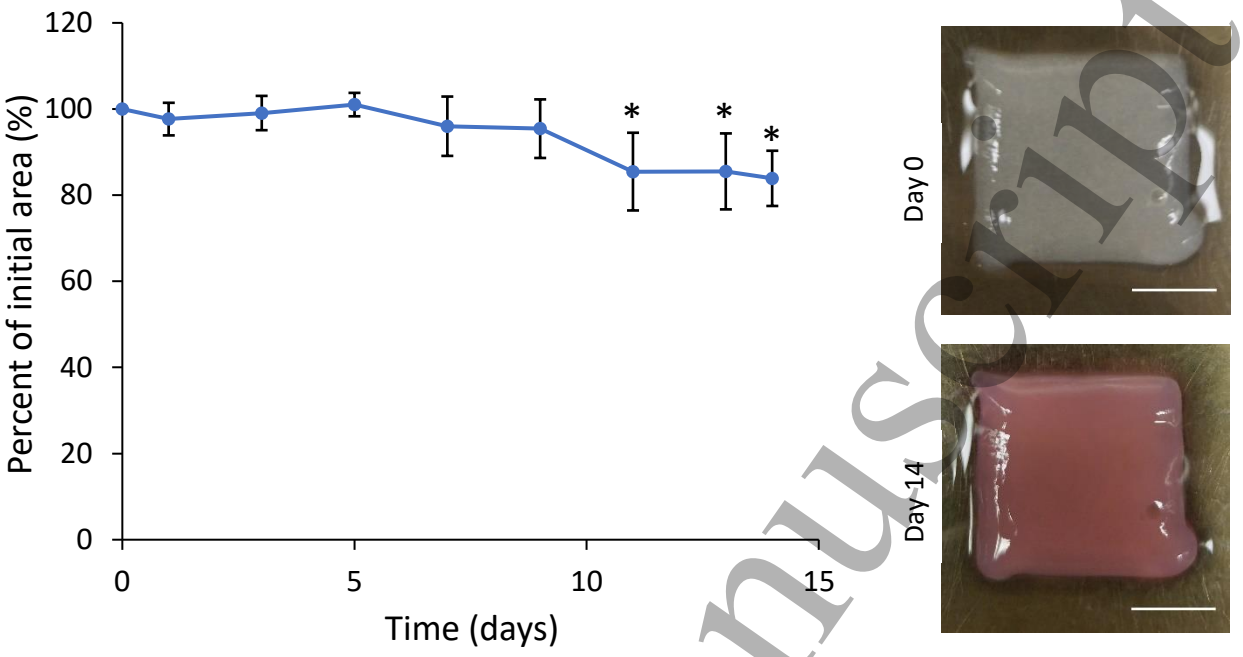

Figure 6. Construct area normalized to area on day 0 with time in culture. All samples fabricated using collagen bioinks with 10 million cells/mL. n = 6 squares per time point. * indicates significant difference from day 0 ($p<0.05$). Top image shows representative image of construct on day 0 and bottom image shows representative image of the same construct on day 14. Scale bars = 10 mm.

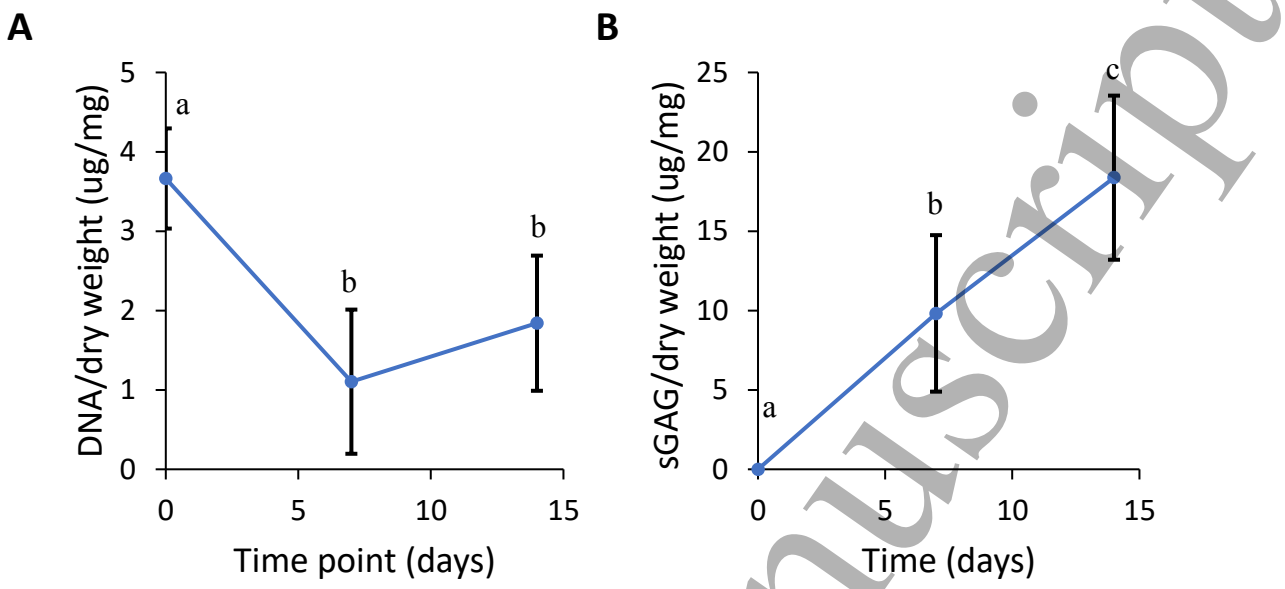

Figure 7. Biochemical analysis of constructs after 0, 7, and 14 days in culture. All samples fabricated using collagen bioinks with 10 million cells/mL. A.) DNA content per dry weight. B.) GAG content per dry weight. n = 7-15 samples per time point. Different letters indicate significant differences ($p<0.05$).

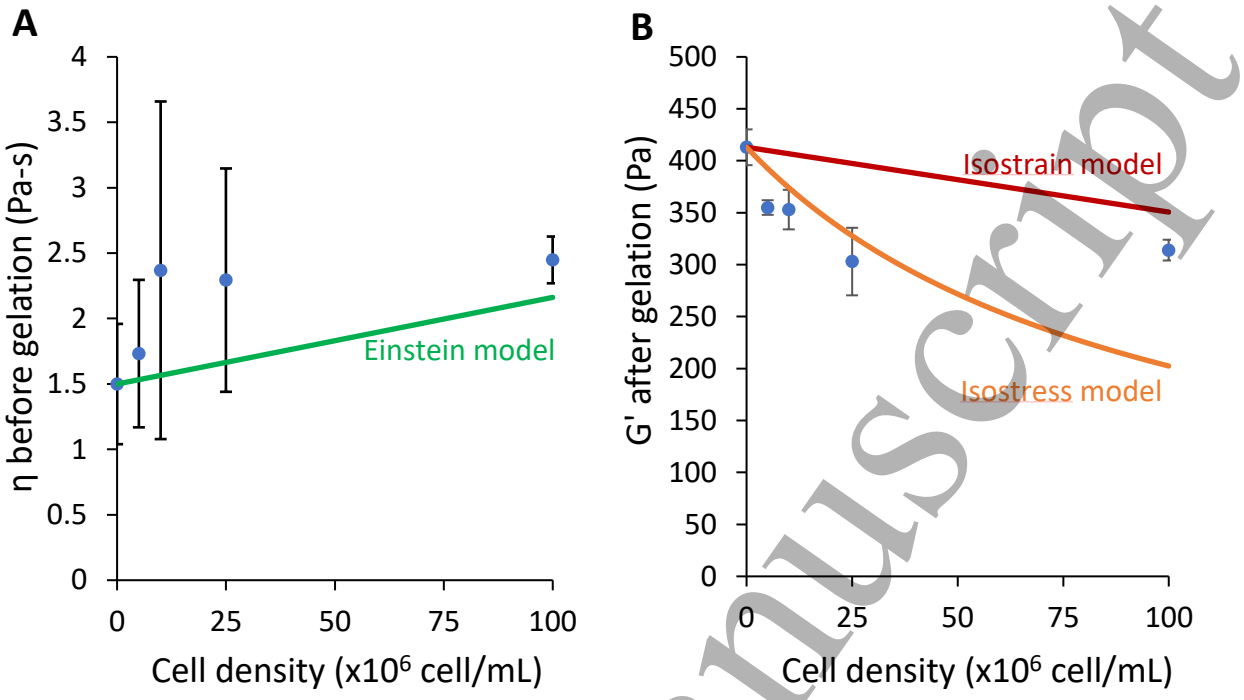

Figure 8. Comparison of rheological findings to models of composite materials. A.) Complex viscosity of collagen solutions before gelation (blue) was best modeled by the Einstein equation (green). B.) Storage moduli of collagen after gelation (blue) for low cell densities were best modeled by the isostress rule of mixtures (orange), whereas the modulus of collagen gels with cell densities of 100 million cells/mL was best predicted by the isostrain rule of mixtures (red). Theoretical models assume chondrocyte diameter of 15 μm and storage modulus of 60 Pa.